JOURNAL OF THEORETICAL AND APPLIED MECHANICS
52, 3, pp. 595-604, Warsaw 2014

DYNAMICAL JUMP ATTENUATION IN A NON-IDEAL SYSTEM THROUGH A MAGNETORHEOLOGICAL DAMPER

Vinicius Piccirillo, Ângelo Marcelo Tusset
UTFPR – Federal Technological University of Paraná, Department of Mathematics, Ponta Grossa, Brazil
e-mail: piccirillo@utfpr.edu.br; a.m.tusset@utfpr.edu.br

José Manoel Balthazar
UNESP – São Paulo State University, Department of Statistics, Applied Mathematical and Computation, Rio Claro, Brazil
e-mail: jmbaltha@gmail.com

This paper is concerned with the Sommerfeld effect (Jump phenomena) attenuation in an non-ideal mechanical oscillator connected with an unbalanced motor excitation with a limited power supply (non-ideal system) using a magnetorheological damper (MRD). The dynamical response of systems with MRD presents different behavior due to their nonlinear characteristic. MRD nonlinear response is associated with adaptive dissipation related to their hysteretic behavior. The Bouc-Wen mathematical model is used to represent the MRD behavior. Numerical simulations show different aspects about the Sommerfeld effect, illustrating the influence of the different electric current applied in the MRD to control the force developed by this damper.

Keywords: magnetorheological damper, Sommerfeld effect, nonlinear dynamics

1. Introduction

In the study of problems that involve coupling of several systems, changes of structural characteristics of machines and their component have been investigated in the recent years. In this way, some phenomena are observed in composed dynamic systems suporting structures and rotating machines, in which it has been verified that the unbalancing of rotating parts is the major cause of vibrations. In the study of such systems, for a more realistic formulation one must consider the action of an energy source with a limited power (non-ideal), that is consider the influence of the oscillatory system on the driving force and vice versa. Recently, a number of works have been done in order to investigate resonant conditions of non-ideal vibrating oscillator systems (Balthazar *et al.*, 2003) and a number of several non-ideal vibrating systems has been studied, for some examples (Frolov and Krasnpolskaya, 1987; Krasnopolskaya and Shvets, 1994; Piccirillo *et al.*, 2009, 2011; Tusset and Balthazar, 2013) and many others.

The Sommerfeld effect is a kind of problem that occurs in non-ideal systems near resonance frequencies. This effect was described in the classical book byKononenko (1969), entirely devoted to this subject. The jump phenomena in the vibration amplitude and the increase of the power required by the source to operate next to the system resonance are both manifestations of this non-ideal problem. This phenomenon suggests that the vibratory response of the non-ideal system emulates an "energy sink" in the regions next to the system resonance, by transferring the power from the source to vibrations of the supporting structure instead of the speeding up the driving machine (Castão *et al.*, 2010). In other words, one of the problems confronted by mechanical engineers is how to drive a system through the system resonance and to avoid this "disappearance of energy" as originally described by Sommerfeld (Nayfeh and Mook, 1979).

Palacios *et al.* (2009) presented a research which contained analysis of the Lugre friction in elimination of the Sommerfeld effect for a non-ideal structural system (NIS). The authors

observed significant reductions in the resonance capture phenomenon when this friction law is considered in NIS and consequently, the Sommerfeld effect is then eliminated. The analysis of the Sommerfeld effect of a Duffing-Rayleigh oscillator under a non-ideal excitation (unbalanced motor with a limited power supply) using the method of averaging and numerical computation was investigated by Felix *et al.* (2009a). Furthermore, for the reduction of the Sommerfeld effect, the jump phenomenon and resonance capture there was used a shape memory alloy spring. According to Belato (1998), the jump phenomenon related to the Sommerfeld effect is associated with a cyclic saddle-node bifurcation with the system losing its stability in the point where the jump occurs.

In this work, we use a semi-active approach to reduce resonance vibrations of a non-ideal structure (Sommerfeld effect) in non-ideal system by applying a nonlinear damping with magnetorheological fluids. The mechanism of the damper (MR) is similar to the mechanism of hydraulic dampers in which the force is obtained by passage of the fluid through an orifice. This variable resistance to fluid flow allows using a viscous fluid in MR dampers and other devices electrically controllable. Thus, the magnetic properties of the fluid allow its use as a damper controlled by electric voltage (V) or an electric current (A) (Tusset *et al.*, 2009).

The use of MR damper control in the suppression of unwanted oscillations is done by the electrical current or voltage which changes the viscosity of the internal damper fluid. The damping force will depend on the velocity of the piston of the damper and density of the internal fluid.

2. Magnetorheological damper model with hysteresis

The MRD is a semi-active device inwhich the viscosity of the fluid can be controllable by a change in the input voltage (Spencer *et al.*, 1997). A large number of analytical models based on different descriptions have been done with the objective of describing nonlinear properties of MR dampers. The force-velocity characteristics of the MRD measured after various excitations and electric currents, indicates nonlinear behavior such as hysteresis (Ma *et al.*, 2003).

The velocity of the piston also has an important influence on the dynamic properties of the MRD fluid. If the velocity is high, the duration in which the particles are in the magnetic field is short. This results in saturation of the damping force to the upper velocity $\pm 0.4\,\mathrm{m/s}$. Saturation can also occur in relation to the applied electric current in the coil with electric currents between 0 and 1.5 A. (McManus *et al.*, 2002).

Bouc-Wen model of the MR damper

A large number of models of MRDs have been proposed for describing their hysteretic behavior (Wang and Liao, 2011), such as bi-viscous model, Bouc-Wen model, neural-network-based model, etc. A model that can be solved numerically and used to represent the MRD dynamics with hysteresis is the Bouc-Wen model. The Bouc-Wen model is considered to be extremely versatile and can display a wide variety of hysteretic behavior. Figure 1 shows the layout of the Bouc-Wen model (Dominguez *et al.*, 2006).

The force F of the system is determined by

$$F = c_0\dot{x} + k_0 x + \alpha z \tag{2.1}$$

and z is obtained from the equation

$$\dot{z} = -\varsigma|\dot{x}|z|z|^{n-1} - \xi\dot{x}|z|^n + \Lambda\dot{x} \tag{2.2}$$

This Bouc-Wen model incorporates the MR damper force f_0 as an initial displacement x_0 and a stiffness coefficient k_0. It can be seen in Eqs, (2.1) and (2.2) that the control variable (i)

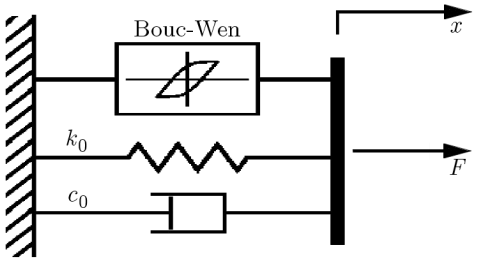

Fig. 1. Bouc-Wen model of the MR damper

does not appear explicitly. Since the goal is to control the damper strength using the electric current, an approximation of Eq. (2.1) can be used that depends explicitly on the electric current (Tusset *et al.*, 2013)

$$F = \frac{3.2}{3\mathrm{e}^{-3.4i}+1}\dot{x} + k_0 x + \frac{8.5}{1.28\mathrm{e}^{-3.9i}+1}z \tag{2.3}$$

The electrical current to be applied can be determined by solving numerically the following function (Tusset *et al.*, 2013)

$$C(i) = \frac{3.2}{3\mathrm{e}^{-3.4i}+1}\dot{x} + k_0 x + \frac{8.5}{1.28\mathrm{e}^{-3.9i}+1}z - F \tag{2.4}$$

In order to examine the response of the MRD, a comparison with Eq. (2.1) proposed by Dominguez *et al.* (2006) with Eqs. (2.3) and (2.4) proposed by Tusset *et al.* (2013) has been made, and this comparison is very close, as can be seen in Fig. 2. The characteristics of variation of the damping force dependingon the velocity of the piston of the damper and the applied electric current in the coil estimated for an excitation of 1 Hz and an amplitude of 0.04 m, with the parameters $\Lambda = 180$, $k_0 = 0$, $\xi = 0$, $n = 2$, $\varsigma = 0.1$ and Table 1 (Yao *et al.*, 2002).

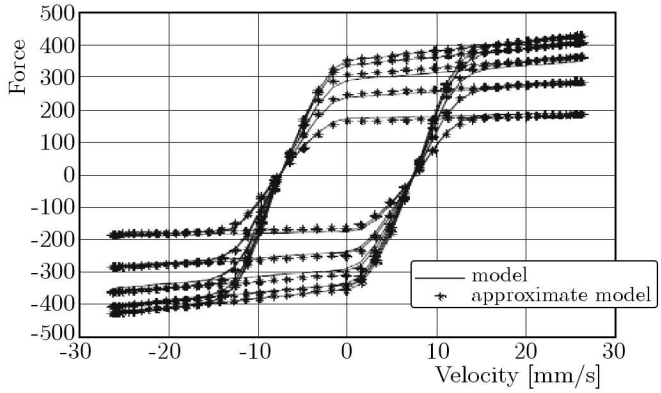

Fig. 2. Characteristics of the MR damper as function of the electric current considering the model by Dominguez *et al.* (2006) and the model by Tusset *et al.* (2013)

Table 1. System parameters used in Fig. 2 (Yao *et al.*, 2002)

Electric current i	Parameter c_0	Parameter α_0
0	1.00	5.630
0.25	1.65	4.102
0.50	2.20	6.877
0.75	2.50	7.950
1.00	2.90	8.300

3. Non-ideal excitation

Let us consider a vibrating system (NIS) which includes a direct current (DC) motor with a limited power supply operating on a structure (Fig. 3). The excitation of the system is limited by a characteristic of the energy source (non-ideal energy source). Then, the coupling of the vibrating oscillator and the DC motor takes place. As the vibration of the mechanical system depends on the DC motor, also motion of the energy source depends on vibrations of the system. Hence, it is important to analyze what happens to the motor as the response of the system changes.

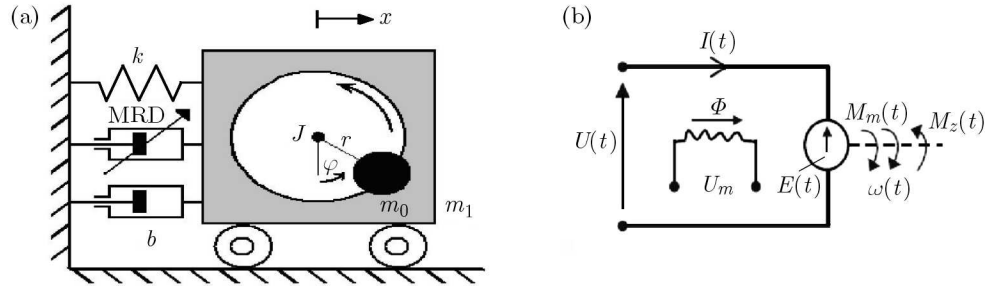

Fig. 3. (a) Non-ideal mechanical system (NIS) and (b) electrical schematic representation of the DC motor

The considered vibrating system consists of a mass m_1, linear damping with viscous damping coefficient b. The non-ideal DC motor has the driving rotor of moment of inertia J, and r is the eccentricity of the unbalanced mass.

The electrical scheme of the DC motor is presented in Fig. 3b. The equations governing the motion of the DC motor are typically written in the form by Warminski and Balthazar (2003)

$$J\frac{d^2\varphi}{dt^2} = M_m(t) - M_z(t) - H(t) \qquad U(t) = R_t I(t) + L_t\frac{dI(t)}{dt} + E(t) \tag{3.1}$$

where time functions $U(t)$ and $I(t)$ are the voltage and current in the armature, R_t and L_t is the resistance and inductance of the armature, $E(t)$ is the internally generated voltage, $M_z(t)$ is the external torque applied to the motor driving shaft, $H(\varphi)$ is the frictional torque and $M_m(t)$ denotes the torque generated by the motor. The torque $M_m(t)$ and internal generated voltage $E(t)$ can be expressed as

$$M_m(t) = c_M \Phi I(t) \qquad E(t) = c_E \Phi \omega(t) \tag{3.2}$$

where c_M, c_E are mechanical and electrical constants, and Φ is the magnetic flux. Let us assume that the external exciting current I_m and voltage U_m are constant, and then the magnetic flux Φ is also constant in the considered model. Taking into account Eqs. (3.1) and (3.2), we can write differential equations of the complete electro-mechanical system presented in Fig. 3 as follows

$$\begin{aligned} &Mx'' + bx' + F + k_l x + k_{nl}x^3 - m_0 r(\varphi'^2 \sin\varphi + \varphi'' \cos\varphi) = 0 \\ &(J_M + m_0 r^2)\varphi'' = c_M \Phi \widetilde{I}(t) - \widetilde{H}(\varphi') + m_0 r x'' \cos\varphi \\ &\frac{d\widetilde{I}(t)}{dt} = -\frac{R_t}{L_t}\widetilde{I}(t) - \frac{c_E \Phi}{L_t}\varphi' + \frac{\widetilde{U}(t)}{L_t} \end{aligned} \tag{3.3}$$

where the prime denotes the derivative with respect to dimensional time and $M = m_1 + m_0$, and F is the MRD restoring force. It is convenient to work with the dimensionless position and time, in such a way that Eqs. (3.3) are rewritten in the following form

$$\begin{aligned} &\ddot{u} + \zeta\dot{u} + F_{MRD} + u + \gamma u^3 - w_1(\dot{\varphi}^2 \sin\varphi + \ddot{\varphi}\cos\varphi) = 0 \\ &\ddot{\varphi} = p_3 I(\tau) + w_2 \ddot{u}\cos\varphi - H(\varphi) \qquad \dot{I} = U(\tau) - p_1 I(\tau) - p_2\dot{\varphi} \end{aligned} \tag{3.4}$$

where

$$\omega_0^2 = \frac{k_l}{M} \qquad \zeta = \frac{b}{M\omega_0} \qquad \gamma = \frac{k_{nl}}{k_l}x_{st}^2 \qquad I = \frac{\widetilde{I}}{I_r}$$

$$w_1 = \frac{m_0 r}{M x_{st}} \qquad w_2 = \frac{m_0 r x_{st}}{J + m_0 r^2} \qquad p_1 = \frac{R_t}{L_t \omega_0} \qquad p_2 = \frac{c_E \Phi}{L_t I_r}$$

$$p_3 = \frac{c_M \Phi I_r}{(J + m_0 r^2)\omega_0^2} \qquad U(\tau) = \frac{\widetilde{U}(\tau)}{L_t I_r \omega_0} \qquad H(\varphi) = \frac{\widetilde{H}(\varphi')}{(J + m_0 r^2)\omega_0}$$

$$\tau = \omega_0 t \qquad u = \frac{x}{x_{st}} \qquad F_{MRD} = \frac{F}{M\omega_0^2 x_{st}}$$

and x_{st} means the static displacement of the system, τ is the dimensionless time, I_r is rated current in the armature and dots indicate differentiations with respect to the dimensionless time, the function $H(\varphi)$ is the resistive torque applied to the motor and, in this work, $H(\varphi)$will be neglected $(H(\varphi) = 0)$.

4. Results of numerical simulation

This section considers numerical simulations that are meant to illustrate the MRD influence on jump phenomena in a complete electro-mechanical system. The DC motor and mechanical parameters used in numerical simulations are given in Table 2. All simulations consider the following oscillator parameters: $R_t = 1\,\Omega$, $L_t = 3.7 \cdot 10^{-2}\,\mathrm{H}$, $I_r = 3.93\,\mathrm{A}$, $c_E\Phi = 0.437\,\mathrm{Vs/rad}$, $c_M\Phi = 0.437\,\mathrm{Nm/A}$.

Table 2. System parameters used in simulation (Warminski and Balthazar, 2003)

w_1	w_2	p_1	p_2	p_3	ζ	γ
0.2	0.3	0.3	3	0.15	0.1	0.2

In non-ideal mechanical systems, the oscillator cannot be driven by systems, whose amplitude and frequency are arbitrarily chosen, once the forcing source has a limited available energy supply. For this kind of oscillator, the driven system cannot be considered as given *a priori*, but it must be taken as a consequence of the dynamics of the whole system (oscillator and motor). Therefore, a non-ideal oscillator is, in fact, a combined dynamical system resulting from the coupling of passive and active oscillators which serve as the driving source for the first ones. The resulting motion will be thus the outcome of dynamics of the combined systems. The dimensionless voltage applied across the armature U is the control parameter in the non-ideal system. For each value of U, the non-ideal system presents one frequency and amplitude behavior.

It is known that the dynamics of a system close to the fundamental resonance region may be analyzed through a frequency-response diagram, which is obtained by plotting the amplitude of the oscillating system versus the frequency of the excitation term. For the complete electro-mechanical system, this graph is estimated by numerical simulation defining the amplitude as the maximum value of the amplitude of mechanical oscillation (denoted by A), and the frequency as the mean value of the rotational speed $\dot{\varphi}$ (denoted by ω).

Figure 4 represents the resonance curve without the MRD device when the mean frequency ω is slowly increased. The curve was calculated using an increment $\Delta U = 0.01$ as the variation of the control parameter U. The transient response is also considered in the computation because its evolution inside the state space determines the occurrence of the jump phenomenon during passage through the resonance region $(\omega \approx 1)$. In Fig. 4a, it can be seen that when the value

of the control parameter is $U \approx 3.1$, the resonance region was reached, so large amplitude vibrations of the system are generated, as shown in Fig. 4b, in other words the system reaches the maximum amplitude of displacement. Note that close to the resonance ($\omega \approx 1$), the power it is supplied to the DC motor to initiate the jump increase (see Figs. 4c and 4d). Then the operating frequency increases and thus the system amplitude decreases resulting in lower power consumption by the DC motor.

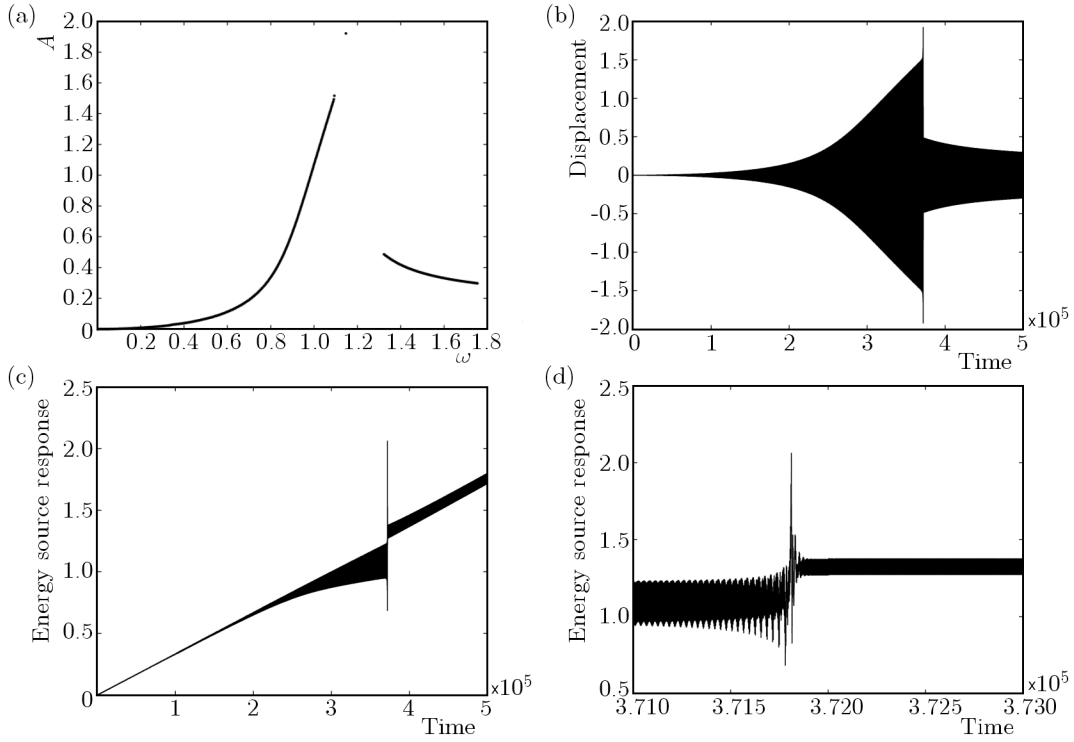

Fig. 4. Jump phenomenon observed when the mean frequency ω is slowly increased: (a) frequency-response diagram without the MRD, (b) time response, (c) energy source and (d) zoom of Figure (c)

The jump phenomenon is characterized by sudden amplitude transition, as indicated in Fig. 4a. This happens because there is not enough damping in the system to stop the DC motor from transmitting large amounts of energy to the nonlinear oscillator. Now, the same non-ideal system is investigated, however, the MRD is introduced in this system, as observed in Fig. 3. The Sommerfeld effect and the MRD parameter in the non-ideal system will be verified, too. These results are compared with the non-ideal system without the MRD. Due to MRD, nonlinear characteristic and dissipative behavior of the jump response tends to exhibit a small vibration amplitude.

When the MRD is introduced to the non-ideal system, it can be observed that for $i = 0A$, that is the electric current applied in the MRD is zero, the reduction of amplitude in the non-ideal system is observed, as shown in Figs. 5a and 5b. Nevertheless, the Sommerfeld effect still happens because the damping introduced by the MRD, in this case, is not efficient to suppress or inhibit the energy transfer from the DC motor to the nonlinear oscillator. Moreover, when compared to the situation with the non-ideal system without an MRD, the MRD non-ideal oscillator presents a smaller amplitude response.

Figure 6 shows the behavior of the non-ideal system with $i = 0.5A$. With this increase in the applied electric current, the characteristics of variation of the damping force change and the Sommerfeld effect starts to be controlled, for this reason the MRD damper dissipates more vibrational energy now than previously, therefore, the amplitude of motion decreases, too.

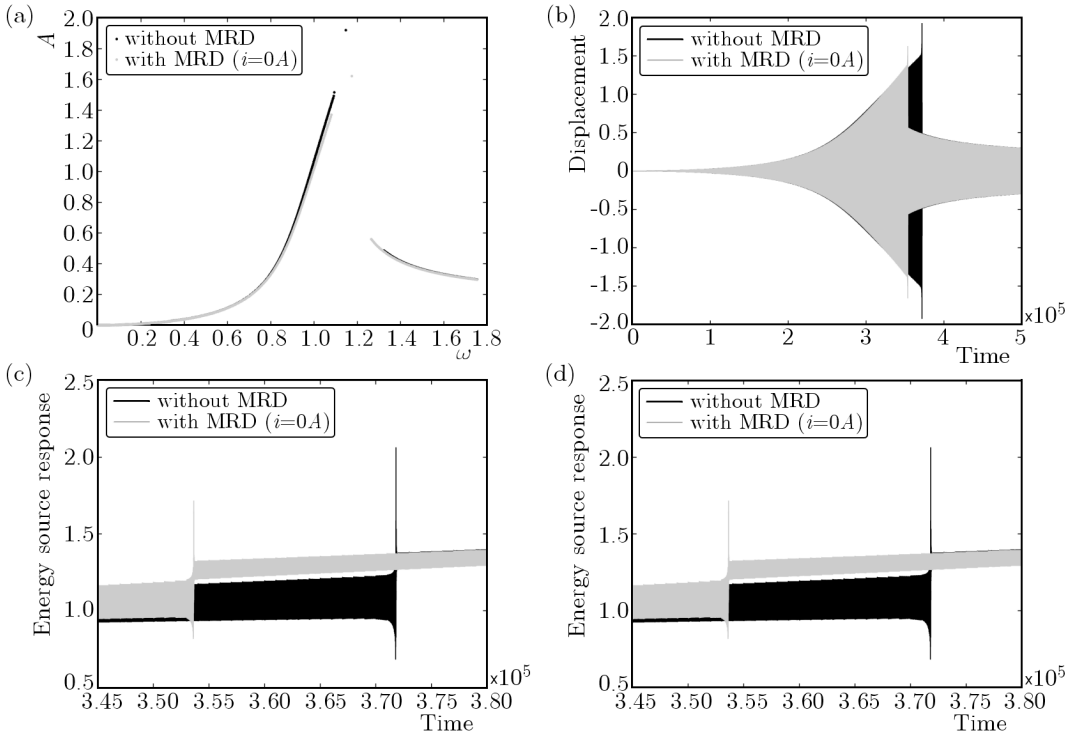

Fig. 5. Jump phenomenon observed when the mean frequency ω is slowly increased: (a) frequency-response diagram with the MRD $(i = 0A)$, (b) time response, (c) energy source and (d) zoom of Figure (c)

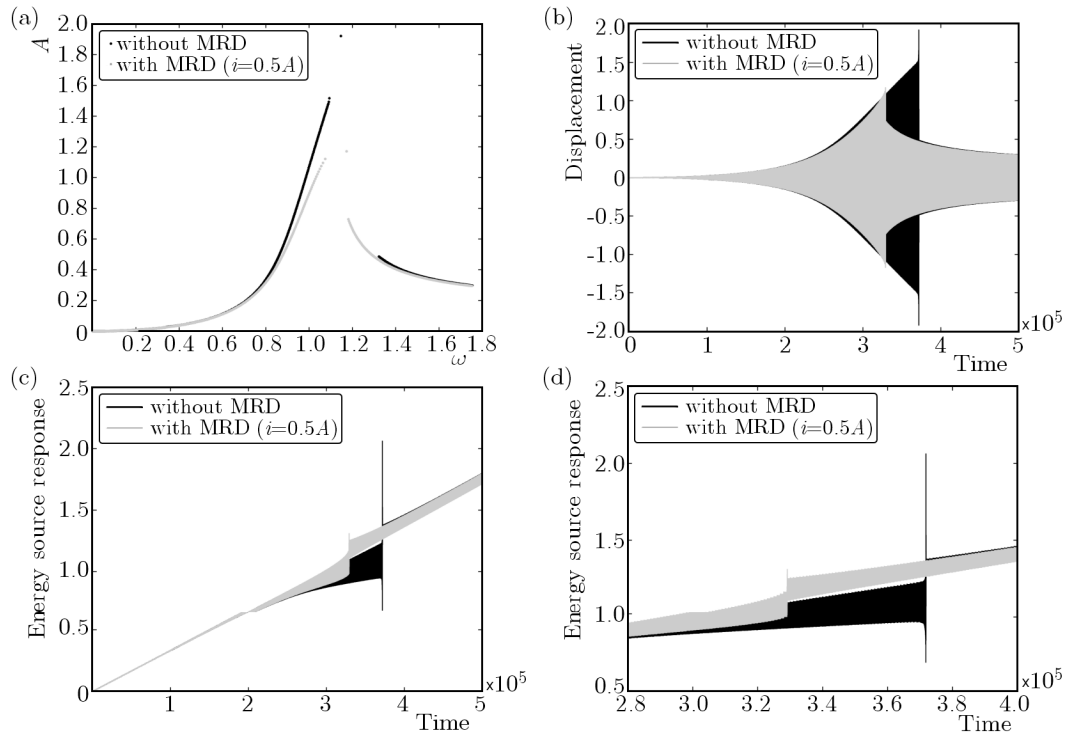

Fig. 6. Jump phenomenon observed when the mean frequency ω is slowly increased: (a) frequency-response diagram with the MRD $(i = 0.5A)$, (b) time response, (c) energy source and (d) zoom of Figure (c)

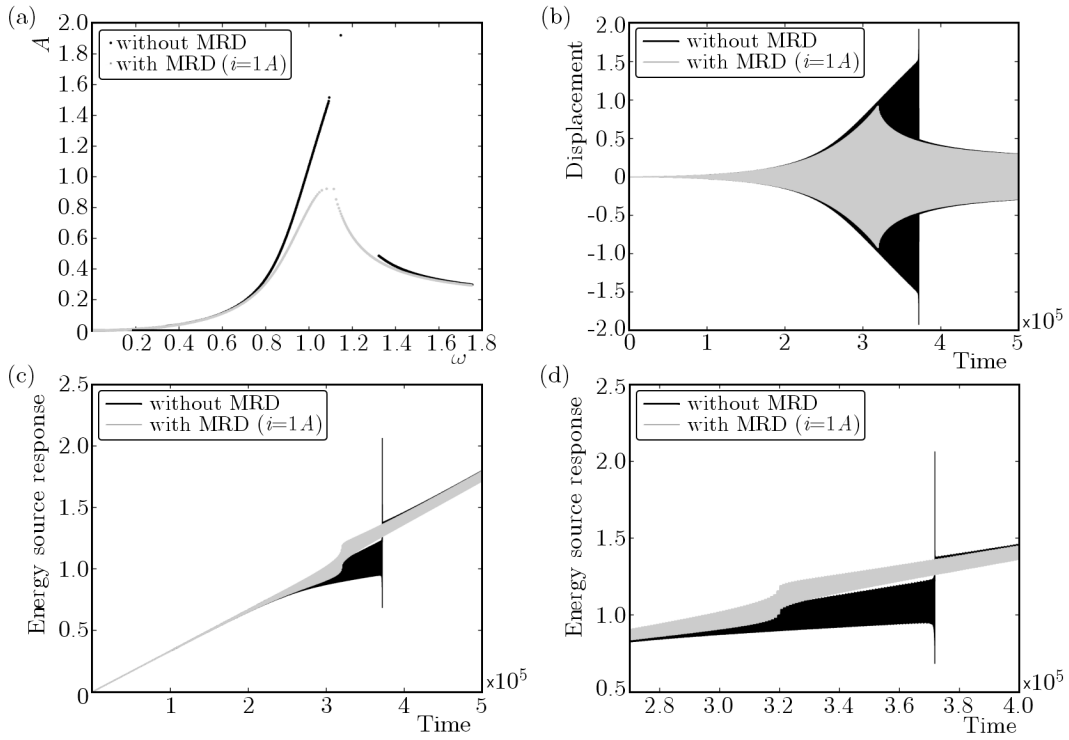

Fig. 7. Jump phenomenon observed when the mean frequency ω is slowly increased: (a) frequency-response diagram with the MRD $(i = 1A)$, (b) time response, (c) energy source and (d) zoom of Figure (c)

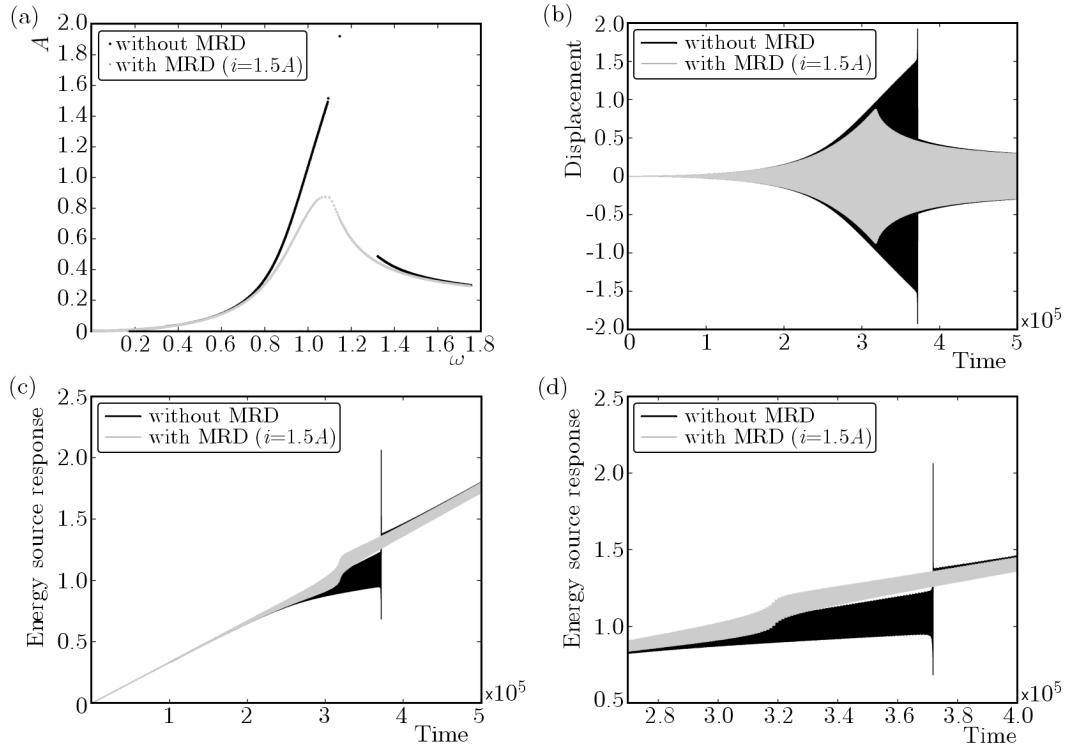

Fig. 8. Jump phenomenon observed when the mean frequency ω is slowly increased: (a) frequency-response diagram with the MRD $(i = 1.5A)$, (b) time response, (c) energy source and (d) zoom of Figure (c)

Figures 6c and 6d show that the energy transferred from the DC motor to the structure began to be controlled, and that meant that the MRD energy dissipation improved (or decrease) the jump.

Figures 7 and 8 show the system, considering that the current is increased to a level of $1A$ and $1.5A$, respectively. In both cases, the Sommerfeld effect is completely put down because the damping force is greater than in the previous cases, and the effect of the MRD results in suppression of the jump phenomena. Note that the increase in the electric current causes a decrease in the amplitude of motion in the resonance region, eliminating possible jumps. In this case, the energy transferred from the DC motor to the oscillator was controlled by means of the MRD.

Figure 9 shows the Sommerfeld effect and its suppression for different values of the electric current. The equivalent non-ideal response is compared with the MRD non-ideal system which allowed one to verify the MRD effect in this dynamical system. It might be observed that the amplitude reduction can be achieved for different electric currents.

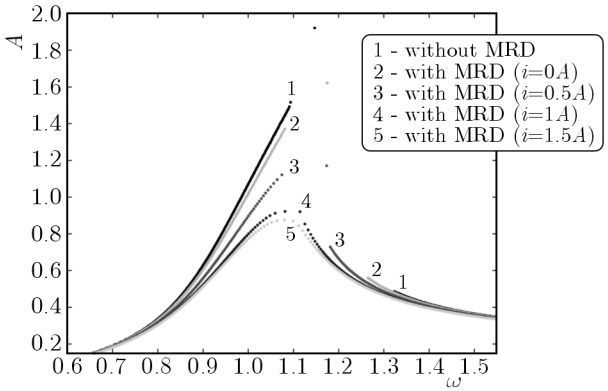

Fig. 9. Jump phenomenon for different values of the electric current

5. Conclusion

In this paper, the attenuation and suppression of the Sommerfeld effect in a non-ideal vibrating system, using an MRD was presented. This happens as a consequence of using an additional electrical current introduced to the MR damper, which increased energy support of the combined system. For this reason, if values of the electric current in the MRD is increased, the damping force grows as well and, therefore, the Sommerfeld effect and the amplitude in resonance regions are avoided. The analysis of this system shows that the introduction of an MR damper, in this case, is efficient to suppress or inhibit the energy transfer from the DC motor to the nonlinear oscillator in resonance cases.

Acknowledgements

The authors acknowledge the financial support by FAPESP and CNPq (grant No. 484729/2013-6).

References

1. Balthazar J.M., Mook D.T., Weber H.I., Brasil R.M.F.L.R.F., Fenili A., Belato D., Felix J.L.P., 2003, An overview on non-ideal vibrations, *Meccanica*, **38**, 613-621
2. Belato D., 1998, Não-linearidades no Eletro Pêndulo, MSc Dissertation, State University of Campinas, Brazil
3. Castão K.A.L., Góes L.C.S., Balthazar J.M., 2010, A note on the attenuation of the Sommerfeld effect of a non-ideal system taking into account MR damper and the complete model of a DC motor, *Journal of Vibration and Control*, **17**, 1112-1118

4. Dominguez A., Sedaghati R., Stiharu I., 2006, A new dynamic hysteresis model for magnetorheological dampers, *Smart Material and Structures*, **15**, 1179-1189
5. Felix J.L.P, Balthazar J.M., Brasil R.M.L.R.F., 2009a, Comments on nonlinear dynamics of non-ideal Duffing-Rayleigh oscillator: numerical and analytical approaches, *Journal of Sound and Vibration*, **319**, 1136-1149
6. Felix J.L.P., Balthazar J.M., Brasil R.M.L.R.F., Pontes Jr B.R., 2009b, On Lugre friction model to mitigate nonideal vibrations, *Journal of Computation and Nonlinear Dynamics*, **4**, 034503-1-034503-5
7. Frolov K.V., Krasnopolskaya T.S., 1987, Sommerfeld effect in system without internal damping, *Soviet Applied Mechanics*, **23**, 1122-1126
8. Konokenko V.O., 1969, *Vibrating Problems with a Limited Power Supply*, Illife, London
9. Krasnopolskaya T.S., Shvets A.Yu., 1994, Chaotic surface waves in limited power-supply cylindrical tank vibrations, *Journal of Fluids and Structures*, **8**, 1-18
10. Ma X.Q., Wang E.R., Rakheja S., Su C.Y., 2003, Evaluation of modified hysteresis models for magnetorheological fluid dampers, *The Fourth International Conference on Control and Automation (ICCA'03)*, Montreal, Canada
11. McManus S.J., St. Clair A., Boileau P.E., Boutin J., Rakheja S., 2002, Evaluation of vibration and shock attenuation performance of a suspension seat with a semi-active magnetorheological fluid damper, *Journal of Sound and Vibration*, **253**, 313-327
12. Nayfeh A.H., Mook D.T., 1979, *Nonlinear Oscillations*, New York: Wiley-Interscience
13. Palacios et al., 2009a, ????????????? (in Introduction)
14. Piccirillo V., Balthazar J.M., Pontes Jr B.R., Felix J.L.P., 2008, On a nonlinear and chaotic non-ideal vibrating system with shape memory alloy (SMA), *Journal of Theoretical and Applied Mechanics*, **46**, 597-620
15. Piccirillo V., Balthazar J.M., Pontes Jr. B.R., Felix J.L.P., 2009, Chaos control of a nonlinear oscillator with shape memory alloy using an optimal linear control: Part II: Non-ideal energy source, *Nonlinear Dynamics*, **55**, 139-149
16. Piccirillo V., Góes L.C.S., Balthazar J.M., 2011, Some remarks on bifurcation analysis of a nonlinear vibrationg system excited by a shape memory material (SMA), *International Journal of Bifurcation and Chaos in Applied Sciences and Engineering*, **21**, 2975-2982
17. Spencer Jr. B.F., Dyke S.J., Sain M.K., Carlson J.D., 1997, Phenomenological model of a magnetorheological damper, *ASCE Journal of Engineering Mechanics*, **3**, 230-238
18. Tusset A.M., Balthazar J.M., 2013, On the chaotic suppression of both ideal and non-ideal Duffing based vibrating systems, using a magneto rheological damper, *Differential Equations and Dynamical Systems*, **21**, 105-121
19. Tusset A.M., Balthazar J.M., Felix J.L.P., 2013, On elimination of chaotic behavior in a non-ideal portal frame structural system, using both passive and active controls, *Journal of Vibration and Control*, **19**, 803-813
20. Tusset A.M., Rafikov M., Balthazar J.M., 2009, An intelligent controller design for magnetorheological damper based on quarter-car model, *Journal of Vibration and Control*, **12**, 1907-1920
21. Wang D.H., Liao W.H., 2011, Magnetorheological fluid dampers: a review of parametric modeling, *Smart Materials and Structures*, **20**, 1-34
22. Warminski J., Balthazar J.M., 2003, Vibrations of a parametrically and self-excited system with ideal and nonideal energy source, *RBCM – Journal of the Brazilian Society Mechanical Sciences*, **25**, 413-420
23. Yao G.Z., Yap F.F., Chen G., Li W.H., Yeo S.H., 2002, MR damper and its application for semi-active control of vehicle suspension system, *Mechatronics*, **12**, 963-973

Manuscript received September 10, 2013; accepted for print December 30, 2013